https://doi.org/10.5194/tc-2022-145
Preprint. Discussion started: 11 August 2022

The Cryosphere Discussions

Effects of extreme melt events on ice flow and sea level rise of the Greenland Ice Sheet

Johanna Beckmann[1] and Ricarda Winkelmann[1,2]

[1]Potsdam Institute for Climate Impact Research, RD1, Potsdam, 14473, Germany,
[2]Institute of Physics and Astronomy, University of Potsdam, Potsdam, Germany

Correspondence: Johanna Beckmann (beckmann@pik-potsdam.de)

Abstract. Over the past decade, Greenland has experienced several extreme melt events, the most pronounced ones in the years 2010, 2012 and 2019. With progressing climate change, such extreme melt events can be expected to occur more frequently and potentially become more severe and persistent. So far, however, projections of ice loss and sea-level change from Greenland typically rely on scenarios which only take gradual changes in the climate into account. Using the Parallel Ice Sheet Model (PISM), we investigate the effect of extreme melt events on the overall mass balance of the Greenland Ice Sheet and the changes in ice flow, invoked by the altered surface topography. As a first constraint, this study estimates to the overall effect of extreme melt events on the cumulative mass loss of the Greenland Ice Sheet. We find that the sea-level contribution from Greenland might increase by 2 to 45 cm by the year 2300 if extreme events occur more frequently in the future, and the ice-sheet area might be reduced by an additional 1500 to 18000 $\mathbf{km^2}$ by 2300 in comparison to future warming scenarios without extremes. We conclude that both changes in the frequency and intensity of extreme events need to be taken into account when projecting the future sea-level contribution from the Greenland Ice Sheet.

1 Introduction

With an ice volume of more than 7 metres sea-level equivalent, the Greenland Ice Sheet (GrIS) is one of the largest potential contributors to global sea-level rise (Morlighem et al., 2017). Since the 1980s, its ice loss has steadily increased with a mass loss increase of 80 Gt/year per decade (Mouginot et al., 2019), making up a significant share of the overall accelerating sea level rise (SLR) (Frederikse et al., 2020). These changes are driven by two main processes: (1) melting and accumulation that influence the surface mass balance (SMB) of the ice sheet and (2) changes in ice dynamics that influence the discharge into the ocean. Both processes have contributed almost equally to recent ice loss (Shepherd et al., 2020), with SMB changes dominating since the year 2000 (Van Den Broeke et al., 2016; King et al., 2020; Slater et al., 2020). There are strong interactions between surface mass balance and ice dynamics, which jointly determine the total future SLR contribution of the GrIS. The decrease in SMB after the year 2000 has been attributed to enhanced melting in summer, which is related to a change of atmospheric circulation patterns over the North Atlantic (negative North Atlantic Oscillation index) (Delhasse et al., 2018). Whether the enhanced runoff was primarily driven by enhanced surface heating (Hofer et al., 2017) or reduced refreezing (Van Tricht et al., 2016) is as of yet unclear.

https://doi.org/10.5194/tc-2022-145
Preprint. Discussion started: 11 August 2022

Simultaneously, an increase of heat waves has been observed in the Northern high latitudes (Dobricic et al., 2020) while the number of extreme cold events declined (AMAP, 2021). This resulted in record breaking temperatures for Siberia in June 2020 (Overland and Wang, 2021) and May 2021 (Sullivan, 2021-11-10).Over Greenland, the cumulative heat wave index, representing the strongest heat wave in a year, has roughly tripled between 1981-1985 and 2011-2015 (Dobricic et al., 2020). Observational data from 2000-2015 shows the probability of a heat wave occurring in the Arctic lies between 5-20 percent (Dobricic et al., 2020), meaning that heatwaves could be experienced roughly every 5 to 20 years in the Arctic.

In the past decade alone, Greenland has been subject to several extreme melt events, particularly in the years 2010 (Tedesco et al., 2011), 2012 (Nghiem et al., 2012) and most recently, during spring/summer 2019 (Tedesco and Fettweis, 2020). These extreme events greatly enhanced the surface mass loss (SMB) of the GrIS and are attributed to a strong negative North Atlantic Oscillation index (NAO) in these summers, that led to persistent anticyclonic pressure heights over Greenland (so-called blocking events) (Hofer et al., 2017; Bevis et al., 2019; Tedesco and Fettweis, 2020).

In 2010, the GrIS experienced an early onset of the melt season with above normal temperatures, that led to a lowering of the surface albedo. Together with persistent warm temperatures and reduced snowfall, the long melt season led to the observed records of surface melt and runoff (Tedesco et al., 2011). Two years later, in 2012, a blocking pressure ridge over Greenland was associated with the extreme event, that melted 98.6% of the ice surface on July 12th, including the summit. For comparison, on average 64.3% of the ice-sheet's surface area were melted between 1981-2010 (Tedesco and Fettweis, 2020). The year 2015 was another anomalous melt year, but the extent was quite different: While in 2012 almost the entire ice sheet was affected by the melt event, the event in 2015 was more localized but unusual since it was centered over the North of Greenland. This northward shift was again controlled by a stagnant pressure ridge in that area (Tedesco et al., 2016).Melting at the summit historically happened every 150 to 600 years and the occurrence in 2012 thus could have been within the natural variability (Nghiem et al., 2012). However, in 2019, the summit melted again and 97% of the ice sheet surface was melted within 3 consecutive days (Tedesco and Fettweis, 2020). Again, a persistent pressure ridge was associated with this melt event, but in contrast to 2012, it transited to the west of the GrIS from Western Europe, where a heat wave was prevailing at the time (Cullather et al., 2020).

With progressing global warming, weather extremes such as these are generally expected to increase in frequency and intensity (Rahmstorf and Coumou, 2011). As of yet, however, it is unclear how such extreme events will affect the overall mass balance and future sea-level contribution from the Greenland Ice Sheet. Typically, the future sea-level contribution is assessed based on a gradual change in climate conditions using numerical 3D ice-sheet models. The models enable us to estimate changes in surface mass balance and ice dynamics in response to different greenhouse gas emission and climate change scenarios. (The joint response of surface mass balance and ice dynamics is termed "full dynamics" throughout this manuscript.)

Based on the CMIP5 (Taylor et al., 2012) model ensemble for the Representative Concentration Pathways (van Vuuren et al., 2011), different studies assess a SLR contribution ranging from 1.5-4.9 cm (Goelzer et al., 2020) for the lowest emission scenario RCP2.6 at the end of the 21st century. For the highest scenario RCP8.5, the SLR contribution from Greenland within the 21st century is estimated at 7-21 cm (Church et al., 2013), 9-13.4 cm (Fürst et al., 2015), 4.6–13 cm (Calov et al., 2018),

https://doi.org/10.5194/tc-2022-145
Preprint. Discussion started: 11 August 2022

14-33 cm (Aschwanden et al., 2019), and 4-14 cm (Goelzer et al., 2020), and for the year 2300, estimates range from 97 to 374 cm (Aschwanden et al., 2019).Although significant SMB changes are detected under global warming in the high-emission scenarios, none of the projections capture the recently observed changes of the negative NAO and the resulting extreme melt events on the Greenland Ice Sheet (Hanna et al., 2008). Moreover, observations show that the overall mass loss from Greenland at present is already higher than projected, which might at least in parts be due to the lack of considering extreme events in the simulations (Slater et al., 2020). If the underlying atmospheric circulation patterns prevail or even intensify in the future, extreme melt events are significantly underestimated in the current projections.

In a first study Delhasse et al. (2018) assesses the potential influence of further extreme melt events on Greenland's SMB, simulating the observed circulation pattern from 2000 until mid of this century. However, the approach was limited to SMB changes only, neglecting the dynamic response of the ice sheet. The effect of future extreme melt events on the total SLR contribution (including changes in SMB and ice dynamics) of the GRIS therefore remains an open question. Here we assess this total contribution, including the changes in ice dynamics, for future extreme events of varying frequency and intensity. The ice dynamics considered in this study are focused on changes of ice flow due to changes in surface gradients and do not consider changes in ocean melt or sliding due subglacial or subglacial processes (see Methods).

2 Methods

To project future mass changes of the GRIS, we use the polythermal and thermomechanically coupled Parallel Ice Sheet Model PISM (University of Alaska Fairbanks, 2019, 2019). We first introduce the model (Sect. 2.1) and describe its model initialization and calibration in Sect. 2.2. For our projection experiments we describe the derivation of temperature forcing scenarios with and without extremes in Sect. 2.3 and the calibration of the surface model to the temperature forcing. Finally, in Sect. 2.4, we present the different experimental settings that allow us to determine the dynamical response of the the GrIS to climate projections with and without extremes.

2.1 Ice Sheet Model PISM

The 3D high-resolution numerical ice-sheet/ice-shelf model includes a hybrid stress balance model (Bueler and Brown, 2009; Aschwanden et al., 2012) that combines the Shallow Ice Approximation (SIA) for vertical deformation (Hutter) and Shallow Shelf Approximation (SSA) for longitudinal stretching (Morland, 1987). The grounding line and calving front can generally move freely. In our experiments the ice sheet is expected to retreat. Thus, ice advance beyond the present-day ice margins is prohibited, by a strongly negative SMB around the ice sheet mask to match the present-day ice sheet extent. In the applied model configuration, we concentrate on the effects of surface mass balance changes (SMB) and submarine melting is kept constant in time. We do not consider changes in ice-ocean interaction via submarine melting as the resolution of most tidewater glaciers would require a finer resolution with a regional setting and we concentrate here on a first constraint for the Greenland wide mass changes. Furthermore, how extreme melt events would translate into ice-ocean interaction is not known and would

https://doi.org/10.5194/tc-2022-145
Preprint. Discussion started: 11 August 2022

be strongly modulated by the englacial and subglacial system of each glacier. Here, these englacial and subglacial processes and their interactions with surface melt are not included. As of yet, many of these processes are not fully understood and their long term effect is unclear (Shannon et al., 2013; Tedstone et al., 2015). The SMB is calculated by a Positive Degree Day (PDD) model (Calov and Greve, 2005) with prescribed surface temperature and precipitation. The projection experiments were run on a 4.5 km grid resolution, a vertical resolution of 20 m and monthly time steps. Bedrock and ice thickness data sets (Morlighem et al., 2017) were used to initialize and calibrate our model. Note that areas with ice thicknesses below 1m are excluded from our analysis. Bedrock deformation was not considered during this experiment.

2.2 Model Initialization and calibration

To obtain a realistic thermodynamic present-day state of the ice sheet, the temperature evolution around Greenland over the last glacial cycle was considered. The spin-up was therefore run over the last 125ka, with a scalar temperature anomaly (same temperature increase for every grid point on the ice sheet) of the 2D climatological mean field (precipitation and surface temperature) of 1971-1990, when the GRIS was close to balance (Mouginot et al., 2019). The historical temperature time series is derived from Oxygen Isotope Records from the Greenland Ice Core Project (GRIP) and can be found in the standard Present Day Greenland NetCDF files (Johnson et al., 2019). The climatological mean field was derived from MARv3.9 with ERA-40 and ERA-Interim of the ISMIP6 project (Fettweis, 2019a). Changes in precipitation were parameterized, with a 7.3% precipitation increase for each degree of surface warming, following previous approaches (Huybrechts, 2002).For computational efficiency we followed the grid refinement by Aschwanden et al. (2016): Starting in SIA-only mode, and a 18 000m grid at -125,000 years, we refined our grid to 9000m at -25,000 years and to 4500m at -5000 years. For the last -1000 years we keep the resolution fixed but added the SSA to the SIA stress regime, for better representation of the fast flowing outlet glaciers. For another improvement in this regard, we linearly altered the friction angle between $5°$ and $40°$ between -700m and 700m of bedrock elevation after Aschwanden et al. (2016). The resulting lower friction for lower altitudes and below sea level leads to an additional increase in surface velocities at the ice sheet margins, resulting in an improved match of flow structure for the glaciers. The state closest resembling present-day Greenland was achieved for the following ice flow parameters: flow enhancement factor E = 3, exponent of the sliding law q = 0.6 and exponent of the flow law for the SSA n = 3. All other parameters we set to default (University of Alaska Fairbanks, 2019, 2019).

The initial state as modelled here has a total ice volume of 7.6 m sea-level equivalent (Fig. 1a). On average, ice thicknesses deviate by 170 m with a root mean square error of 238 m to the observed state. In our initial state the ice thickness is slightly overestimated in the west and underestimated in the east of Greenland compared to observations (Fig. S1). Complete observational velocity data for the entire ice sheet is not available for the time period 1971 to 1990. We therefore compare with the complete velocity data set by Joughin et al. (2018) that gives the average velocities from 1995 to 2015. Our comparison (Fig. S2a,b) shows an overall agreement of the velocity pattern with an average difference between modelled and observed ice speed of 9 metres per year and a root mean square error of 146 metres per year. Stronger deviations occur mainly in the fast flowing glacier regions (Fig. S2c) where the exact position of the glaciers is crucial and a coarse resolution leads to a poorer

https://doi.org/10.5194/tc-2022-145
Preprint. Discussion started: 11 August 2022

agreement with observations (Aschwanden et al., 2016). After reaching the stable spin-up state, our projection experiments were run from the year 1971 onwards.

2.3 Temperature forcing

Starting from an initial state of the Greenland Ice Sheet under present-day boundary conditions (Fig. 1a), we apply surface temperature trajectories based on reanalysis data (Sect. 2.3.1) and the RCP8.5 emission scenario (Sect. 2.3.2). We here choose the RCP8.5 scenario since latest results from satellite observations and regional climate models show that the speed with which Greenland is currently losing ice would only be expected under this highest emissions scenarios (Slater et al., 2020).These are our baseline scenario and we further add extremes of different frequency and intensity (Sect. 2.3.3). After the derivation of the forcing scenarios we calibrate our PDD model to the observed SMB loss (Sect. 2.3.4).

2.3.1 Forcing until 2018

To project the mass changes of the GrIS with PISM, we applied changes in a scalar temperature field derived for the average surface temperature anomaly over Greenland with MARv3.9 (Fettweis et al., 2013, 2017) from ERA (1971-2017) to our spin-up state. We used the ERA Interim data set as it is closest to the observation and includes already some observed extremes. A comparison to observational mass changes (Mouginot et al., 2019) can be found in Fig. S3, showing that our fully dynamic simulations of the ice sheet (red line, Fig. S3) agree reasonably well with the observed mass balance of the GrIS between 1972-2017 (red dashed line, Fig. S3). Our SLR estimates from the SMB-only simulations (see Sect. 2.4) on the other hand lead to a slight underestimation of sea-level rise compared to observations.

2.3.2 Temperature Forcing without extremes

For the temperature evolution without extremes, we use the Greenland-wide averaged surface temperature anomalies as projected by MAR (Fettweis et al., 2013, 2017) based on the MIROC5 RCP8.5 scenario (Fettweis, 2019b) from 2018 until 2100, and extended to the year 2300 (see below, Fig. 2a). Monthly temperature anomalies averaged over Greenland may increase by up to 10 °C by the end of this century (Fig. 2) based on the MIROC5 results. Note that this corresponds to a global mean temperature change of 4 deg by 2100 (Fig. S4); the warming signal over Greenland is significantly stronger due to polar amplification. In July, temperature increases of about 15 °C (Fig. 2) are reached within 2300.

We extended the different scenarios for the 21st century described above until the year 2300: As the MIROC5 output was only available until the year 2100, we derived the annual temperature anomaly for the GRIS until 2300 by interpolating from the emulated annual global mean temperatures (GMT) of MIROC5 by Palmer et al. (2018) (Fig. S4). To this end, from the annual MIROC5 results until 2100 we first derived a quadratic trend function
($\mathrm{T_{GrIS}}$ trend$= 1280.16°\mathrm{C} - 1.31°\mathrm{C/year} \cdot \mathrm{years} + 20°\mathrm{C/year}^{-2} \cdot \mathrm{years}^2$) to exclude the inter-annual variability (Fig. S4a). Together with the GMT until 2100 we determined a fitting function (Fig. S4b)

$\mathrm{T_{GrIS}}$ emulated trend$= 0.1°\mathrm{C} + 0.96°\mathrm{C}^{-1} \cdot \mathrm{GMT} + 0.15°\mathrm{C}^{-2} \cdot \mathrm{GMT}^2$

https://doi.org/10.5194/tc-2022-145
Preprint. Discussion started: 11 August 2022

in order to emulate $\mathrm{T_{GrIS}}$ trend beyond the year 2100 in dependence of the GMT. Thus, with the GMT until 2300 and the fitting function, we established the GrIS trend function until 2300 ($\mathrm{T_{GrIS}}$ emulated trend). To this, we added the inter- and intra- annual variability to receive a more realistic monthly temperature projection. This was done by firstly determining the monthly temperature anomalies to each annual mean value for the years 2050-2100 of MIROC5. In a second step we randomly picked anomaly years of this time frame and added them to our emulated annual trend (T_{GrIS} emulated trend) of 2100-2300 to receive the annual $\mathrm{T_{GrIS}}$ emulated (Fig. S4a). The anomaly years also contain the monthly temperature anomalies and give the MIROC5 monthly temperatures for our experiments until 2300(Fig. 2,grey lines).

The change from a spatially explicit to a uniform temperature forcing adds biases, especially at the margins of the ice sheet. Figure S9 shows a slight overestimation of mass loss at the Western margins in the year 2100 when using uniform forcing. However, the calculated SLR in this case is closer to the original MAR results than when using a 2D temperature field (SI, Fig. S5).

2.3.3 Forcing scenarios with extremes

The MIROC5 temperature trajectory serves as a baseline for the development of the scenarios including temperature extremes. As it is highly uncertain when and at which location exactly extremes are most likely to occur under progressing climate change (Otto, 2016, 2019), we here develop idealized extreme scenarios of different intensities and frequencies: The extremes are added from July 2012 onwards, occurring every 20 (scenario f_{20}), 10 (scenario f_{10}), or 5 (scenario f_5) years, based on the observed heat wave probabilities of 5 to 20 % in the Arctic at present (Dobricic et al., 2020).While in reality extremes occur irregularly, we choose these regular intervals to be able to extract the effect of extreme frequency systematically. The different intensities of our extreme event scenarios are reached by multiplying the 10 year average of MIROC5 temperature anomalies in July by factors of 1.25 (scenario $I_{1.25}$), 1.5 (scenario $I_{1.5}$) and 2 (scenario I_2). We choose to use a multiplier here instead of adding a constant temperature offset, since the magnitude and variability might increase in the future and, e.g., the 2012 extreme event will eventually become the "new normal" under continued global warming in the future. Furthermore, this approach allows us to assess the influence of different intensities in a systematic manner and is easily reproducible for further studies. Section 2.1 in the SI explains in detail how our intensity factors compare to a potential changing climate in the future. With our running mean approach, the factor 1.5 $I_{1.5}$ (Fig. 2) leads to a temperature increase comparable to that of the extreme melt year 2012 ($\Delta \mathrm{T_{ERA}}(2012) = 1.8\ ^\circ\mathrm{C}$, $\Delta \mathrm{T_{I_{1.5}}}(2012) = 1.7\ ^\circ\mathrm{C}$). We therefore use it as the default scenario in this study. Thus $I_{1.25}$ (Fig. S6) and I_2 (Fig. S7) give peak temperatures that lie below and above the observed one in 2012, respectively. In the default scenario, temperatures in July can reach changes of above 20 °C at the ice-sheet surface ($I_{1.5}$, see Fig. 2b). The lower-intensity ($I_{1.25}$) and the higher-intensity (I_2) scenarios lead to temperature increases of around 15 °C and 30 °C respectively (Fig. S6 and Fig. S7). To ensure comparable future SMB calculation between our PDD approach and MAR, we calibrated the PDD model within PISM accordingly.

https://doi.org/10.5194/tc-2022-145
Preprint. Discussion started: 11 August 2022

2.3.4 PDD calibration for future temperature forcing

Since our projections are forced with a scalar temperature field, precipitation changes are determined based on the present-day pattern, modifying it by a precipitation rate parameter. This approach allows different magnitudes of precipitation but does not consider changes in the precipitation patterns themselves. We derived a precipitation rate of 5% per degree of warming, from the weighted monthly mean of the ERA Interim data set for 1971-2018 (Fig. S10).

The PDD model determines the runoff by calculating the melt from snow and ice and the amount which is not refrozen with the refreezing parameter. The default setting leads to a substantial underestimation of the future melt compared to the MAR MIROC5 output. To ensure comparability of future melt changes between the PDD model and the MAR output, we derived a temperature-dependent refreezing parameter from the MAR-MIROC5 daily output. (Fig. S11).

With the determined refreezing parameter, we calibrated our PDD model with the monthly 2D temperature and precipitation fields from MIROC5 until 2100. The closest fit to the MIROC5 SLR via SMB loss was achieved with a temperature standard deviation of $\sigma_{\mathrm{T}} = 5\ ^{\circ}\mathrm{C}$ (Fig. S12). We use the default PDD melt factors for snow and ice of 0.00329 and 0.00879 meters water equivalent per degree per day, respectively. SLR was calculated by the cumulative sum of the SMB anomalies to the 1971-1999 SMB mean.

Thus, all future experiments were run with a precipitation increase of 5% per degree of warming, a temperature standard deviation of 5 °C and a temperature dependent refreezing function of $23.42\% - 1.34\frac{\%}{^{\circ}C} \cdot \Delta T$.

2.4 Experiments for the dynamic response

To quantify the dynamic response of the GrIS we derive ,for each of the future scenarios, three different kinds of SLR-projections:

- (1) Full dynamics: To estimate the total mass loss (SMB and ice dynamics) PISM was run with the temperature scenario and a temperature lapse rate of 6 °C per km which lies in the range of GrIS-wide average lapse rates of the MAR data (Fig. S13).
- (2) SMB-only: To estimate the impacts of SMB changes without any dynamic response from the ice sheet, PISM was run similarly but no dynamic changes were allowed. The SMB changes internally calculated in PISM were converted to mass loss for ice thicknesses above flotation, which in turn gave the projected SLR.
- (3) Dynamics without surface elevation feedback: To approximate the role of the ice sheet dynamics excluding the melt-elevation feedback, PISM was run as in the full dynamics case, but without including the atmospheric lapse rate correction.

For each SLR projection, the control run obtained under fixed boundary conditions was subtracted. The sea-level rise projections for the simulations including ice dynamics was calculated from the PISM variable 'sea-level potential', which gives the potential global sea-level increase if all ice above flotation was melted and distributed as freshwater over the ocean area estimated at $362.5\ 10^6\mathrm{km}^2$. For the SMB-only runs we added the SMB differences from the SMB of the climatological mean

https://doi.org/10.5194/tc-2022-145
Preprint. Discussion started: 11 August 2022

1971-1999 (from our spin-up state) for each grid cell and subtracted the corresponding ice mass change from the thickness above flotation. The calculated ice loss was then converted to sea-level rise equivalent as for the dynamic runs. Since our dynamic control run shows a very slight decrease in ice volume, our spin-up state is not in perfect balance and we therefore subtracted the drift from all simulations.

3 Results

3.1 Additional sea-level rise due to extremes

Based on the temperature scenarios described above, we use the fully-dynamic Parallel Ice Sheet Model PISM (see Methods) to assess the impacts of extreme events on the future sea-level contribution from the Greenland Ice Sheet. This includes changes in the surface-mass balance itself, accelerated flow through the steepening of surface gradients and their interactive feedbacks. We find that under all scenarios, the extreme events generally lead to an increase in ice loss in our model simulations with full dynamics. Compared to the climate change scenario without extremes, the 3.08 m SLR by 2300 determined from MIROC5 is increased to 3.13 m (f_{20}), 3.18 m (f_{10}) and 3.28 m (f_5), or by 1.6 to 6.5 %, for the $I_{1.5}$ scenarios (see Fig. 3a, and Table 2). The lower intensity $I_{1.25}$ scenarios only lead to slightly higher SLR contributions of 3.10 m (f_{20}), 3.12 m (f_{10}) and 3.17 m (f_5) (see Fig. 3b) which is substantially increased for the higher intensity I_2 scenarios with 3.19 m (f_{20}), 3.30 m (f_{10}) and 3.52 m (f_5), respectively (see Fig. 3c). Thus the most severe scenario with extreme events of higher intensity occurring every 5 years (I_2, f_5) results in an increase of projected SLR by almost half a meter compared to the scenario not including extreme events.

The projected sea-level contribution from Greenland is generally much lower within the 21st century, where the climate change scenario without extremes leads to ice loss equivalent to 0.13 m sea-level rise (Table 1). At this order of magnitude, the additional mass loss due to extreme events is not as pronounced as in the year 2300. Only for the higher intensity I_2, we find additional SLR of 1 and 2 cm for frequencies of 10 and 5 years, respectively.

For the same intensity, we further test how long after a particular extreme event significant effects can still be detected in the ice-sheet mass balance. To this end, we apply the forcing including extreme events up until the year 2100 but not thereafter and then compare the respective sea-level responses. Our results suggest that it takes about 20-30 years until the SLR trajectory is closer to its original track (i.e., closer to the MIROC5 scenario) than to the extreme event scenario, and more than 200 years until the effect from the extreme events is diminished to less than 10 %. With the preceding $\mathrm{I}_2, \mathrm{f}_5$ extreme scenario until 2100, the final SLR by the year 2300 without continued extremes is 3.09 m, almost equal to the MIROC5 scenario (3.08m).

https://doi.org/10.5194/tc-2022-145
Preprint. Discussion started: 11 August 2022

3.2 Importance of ice dynamics

In order to quantify the relative importance of ice-sheet dynamics, we compare the full-dynamic simulations conducted with PISM to SMB-only simulations, keeping all other parameters fixed (Sect. 2.4). Including ice-dynamic effects generally increases the projected ice loss from Greenland (Fig. S14 and S15, see also Tables 1 and 2), as the dynamical ice flow transports ice from the interior towards the margins of the ice-sheet, thus delivering more ice to the ablation zone where it can subsequently melt. Furthermore, enhanced surface melt can eventually onset the melt-elevation feedback, where the lowered surface elevation exposes the ice to warmer temperatures, in turn leading to more melting.

Based on the MIROC5 results, the SMB-only scenario leads to SLR of 0.08 m by 2100, which increases to 0.13 m when including ice dynamics. Neglecting the melt-elevation-feedback would result in a total of only 0.11 m SLR, i.e., 2 cm less than when considering the full dynamics (see Table 1). For the I_2, f_5-SMB only scenario we experience an average yearly increase of SMB loss of a factor 1.2 (Table S1) compared to the baseline SMB-only scenario in the time frames 2012-2037 and 2038-2048 when average summer temperature (in the base line scenario) is increased by 1.5 and 2 °C respectively (Fig. S16). This shows that our extreme scenarios are rather conservative for this time period compared to the doubling of SMB found in a previous study (Delhasse et al., 2018).

The amplification of the sea-level response due to ice dynamics is pronounced even more in the extended projections until the year 2300: For our Mirco5 simulations, the SMB-only scenario leads to SLR of 2.27 m, while the full-dynamic response of the GrIS yields 3.08 m SLR in our simulations, translating into a 35 % increase compared to the SMB-only scenario (Table 2). The same dynamic enhancement occurs for the extreme event scenarios, where the full-dynamic simulations result in higher sea-level projections compared to the SMB-only case (see Tables 1 and 2). This clearly shows the importance of including both effects from surface-mass balance and the ice dynamics in sea-level projections in an interactive manner.

Overall, the effect of including ice dynamics is greater than the increase between the different extreme event scenarios considered here (Fig. S14 and S15), further underlining how crucial it is to assess the full dynamic response of the GrIS, including impacts with respect to ice retreat and changes in ice velocity.

3.3 Ice-margin retreat and velocity changes

Ice loss primarily happens at the margins of the ice sheet, were melting is more prominent and temperatures are higher due to the lower surface elevations than in the ice-sheet interior. As the topography is lower in the west than the east of Greenland, the west is generally also more exposed to higher surface temperatures and more vulnerable to the melt-elevation feedback. Consequently, in our simulations we find the strongest retreat and decline in ice area in Western Greenland as well (Fig. 1b). To describe the differentiated behaviour of the ice sheet, we introduce different basins (Rignot and Mouginot, 2012; IMBIE2016, 2019): North(NO), North-East(NE), South-East(SE), South-West(SW),Central-West(CW) and North-West(NW) as depicted in Figure (1). The South-West region shows the furthest retreat (Fig. S17,Fig. S18) with a total ice loss of $258\ 10^3$Gt by 2300

https://doi.org/10.5194/tc-2022-145
Preprint. Discussion started: 11 August 2022

(Fig. S18). Approximately the same amount is lost in the North-East region (Fig. S18), but constitutes only a smaller fraction of its present-day ice volume (Fig. S19).

In total, the Greenland Ice Sheet loses about $298\ 10^3\mathrm{km}^2$ of ice area by 2300 in the scenario without extreme events (Table S2), that is approximately 14 % of its area at present ($2136.86\ 10^3\mathrm{km}^2$, see Fig. 1a).

This area is further reduced by 3000 and $5000\ \mathrm{km}^2$ for extremes occurring every 20 and 10 years (for the default $I_{1.5}$ scenario, see Table S2). For increased frequencies, with extreme events occurring every 5 years ($I_{1.5}, f_5$) the ice-sheet area is reduced by an additional 9000 km^2, resulting in a more pronounced ice retreat at the margins of the Greenland Ice Sheet (Fig. 1b). The lower intensity $I_{1.25}$ scenarios lead to less additional area losses of only half the ones detected for $I_{1.5}$, while extremes with the highest intensities I_2 approximately double the additional area loss.

At the same time, the reduced ice area in 2300 is accompanied by an acceleration of ice velocities from an average $25\ \mathrm{m/year}$ to $52\ \mathrm{m/year}$ (for the $I_{1.5}, f_5$ case, see Fig. 1d). Areas where the ice velocities are faster than $100\mathrm{m/year}$ comprise roughly 18% of the Greenland Ice Sheet by 2300 in our simulations. This corresponds to an increase by a factor of 1.5 compared to the initial state (where roughly 12% of the ice flows this fast (Fig. S20). However, in the year 2300, glaciers with maximum velocities higher than 500m per year are lost due to the overall ice retreat (Fig. S20,S21). Changes of the ice sheet differ for specific regions. The average ice sheet wide speedup is therefore mainly caused by a moderate speedup of the ice area around the catchment areas of the glaciers (Fig. 1d) and the continuous speedup of the CW sector (Fig. S22). The CW-sector is the only sector in which average surface velocities continue to increase until 2300 (Fig. S23). The acceleration can be attributed to an increased gravitational driving stress, which is a function of the ice thickness and surface gradients. The speedup of the CW-sector throughout the warming scenario is driven by a strong steepening in surface slope that counteracts the overall thinning, thus increasing the driving stress (Fig. S24). The SW sector also experiences a steepening of its ice surface (Fig. S24). The average thinning however, diminishes this effect on the driving stress and thus surface velocities increase only moderately until 2250 (Fig. S23). After 2250 very little ice remains in the SW-sector, leaving only slow-flowing ice close to the summit. Surface steepening also leads to a small speedup in the NE until 2300 and the NO until 2200, where thinning then results in a decrease in driving stress and subsequent slowdown. The NW and the SE sector both experience a deceleration of surface velocities until 2300 due to a decrease in driving stress. While this is due to a decrease in surface slope and even thickening in the SE-sector until around 2200, the NW sector steadily thins, leading to the decrease of driving stress. Overall we find lower average sector velocities with increasing intensity of extremes (Fig. S25) due to the additional thinning and reduced driving stress induced by the enhanced SMB loss.

3.4 Role of intensity and frequency of extreme events

Our results show that extreme events can add considerable mass loss to existing projections from Greenland. Herein, both the intensity and frequency of the extreme events play a crucial role in determining the future evolution of the ice sheet (Fig. 4): In our model simulations with full dynamics, a doubling in frequency leads to twice as much additional SLR for all intensities. At the same time, increasing the intensity from 1.25 to 2, enhances the additional ice loss by roughly a factor of 5. In combination,

https://doi.org/10.5194/tc-2022-145
Preprint. Discussion started: 11 August 2022

a higher frequency and intensity have an even stronger effect than their sum.

Considering solely the changes in SMB, we find a similar relationship, with relative ice loss doubling for a doubling in frequency, and increasing by a factor of 5 for a change in intensity from 1.25 to 2 (Fig. S26). Thus the relative changes of the SMB-only and the full dynamic run are approximately the same (Fig. S27 and S28). The dynamic run without the surface-elevation feedback adds an additional 3-4cm in 2300 to the SMB-only scenario regardless of the intensity of the extreme (see Table 2). Once more, this highlights the importance of the surface-elevation feedback, which further amplifies the effect of the extreme events on the SLR contributions.

Discussion

Overall, we find that along with progressing climate change, the more frequent occurrence of extreme events plays a crucial role in determining the future sea-level contribution of the Greenland Ice Sheet. Our results suggest that over time, extreme events can lead to an additional retreat of the ice-sheet margins and additional ice volume loss compared to the baseline climate change scenario. Taking severe extreme events (I_2, f_5) into account can increase the projected sea-level rise by up to half a meter by the year 2300 compared to the MIROC5 scenario without additional extremes. Thereby, both the intensity and frequency of the extremes play an equally important role. Compared to the baseline scenario, surface velocities in turn can decrease when including more intense extreme events, due to the reduced driving stress invoked by the additional SMB loss and thinning.

3.4.1 Comparison to other studies

The importance of considering extremes in future projections of the Greenland Ice Sheet is further supported by other studies (Mikkelsen et al., 2018), that show a strong effect of temperature variability on the GrIS equilibrium volume. The experiments conducted here are rather conservative (at least on the short term) in the sense that the simulated SMB loss only increases by a factor of 1.2 and not 2 as for instance in a previous approach by Delhasse et al. (2018) when increasing the average summer temperature by 1.5 °C (mean of summers from 2017-2036) and 2 °C (mean of summers from 2028-2047) above the 1990-1999 summer temperature mean. This can be attributed to the fact that the previous approach re-simulated the total summer variability of 2000-2017, while we here only increase the variability in July by extremes. Figure S16 demonstrates the substantial increase of 0.7-0.8 °C in summer mean temperatures (on top of the average 1.5 °C and 2 °C), if we were to add the variability of the summers in 2000-2016 as from ERA observations (Dee et al., 2011). While this approach would lead to more SMB loss in the time frame until 2050, increases in variability would not be considered and lead to lower SMB losses on longer time scales compared to our approach.

For the year 2100, our projected SLR without extremes of 13cm lies in the upper range of other estimates (Fürst et al., 2015; Calov et al., 2018; Goelzer et al., 2020) and well within the estimates in the 6th Assessment Report of the IPCC(Fox-Kemper and Yu, 2021) of 9-18cm for SSP5-8.5. Only our simulations with extremes match the lower range of Aschwanden et al. (2019)

https://doi.org/10.5194/tc-2022-145
Preprint. Discussion started: 11 August 2022

(14-33cm) for the year 2100. In the same study the optimal simulation, that best reproduced the 2000–2015 mean surface mass balance, led to an estimated SLR of 174 cm in 2300 with an uncertainty range of 97-374 cm(Aschwanden et al., 2019). Our simulations without (308cm) and with extremes (352cm) lie thus in their upper uncertainty range.

3.4.2 Limitations

In this study, we looked at Greenland-wide heat events with a spatially uniform temperature increase, potentially adding a bias of higher mass loss at the western margins of the ice sheet (until the year 2100, where 2D data was available for comparison) compared to a use of the spatially distributed temperature changes. Future work could concentrate on more local melt events and the vulnerability of specific regions in Greenland. Our simulations do not include effects from ice-ocean interaction which may play a crucial role with respect to the dynamic changes of glaciers at the margins of the GrIS (Beckmann et al., 2019; King et al., 2020). Further, we here use a PDD model to simulate changes in the surface mass balance, which is only temperature-dependent and does not consider changes in humidity, radiation, pressure or albedo like the more complex energy balance models (Krebs-Kanzow et al., 2018) or regional climate models (Fettweis et al., 2017; Noël et al., 2018). Likewise, potential changes in precipitation patterns were neglected and only temperature-dependent changes in precipitation (based on the pattern from 1971-1990) included. Our experimental setup generally shows an enhanced sensitivity towards the surface elevation feedback. For the years 2100 and 2300 we detect a 18% and 33% increase of SLR from the dynamic simulations without and with the surface elevation feedback. Other experiments using one-way coupling of regional climate model MAR and an ice sheet model, where the SMB changes are calculated with MAR, show an increase of 4% in 2100 (Edwards et al., 2014), 8% in 2150 (Le Clec'h et al., 2019) and 10% in 2200 (Edwards et al., 2014)) when the surface-elevation feedback is considered.

4 Conclusions

Despite these limitations however, the PDD model parameters were tuned to best match the SMB evolution calculated by regional climate model MAR, and our SLR projections based on the scenario without extremes lie within the same order of magnitude compared to former projections until year 2100 (Fürst et al., 2015; Calov et al., 2018; Goelzer et al., 2020) and 2300(Aschwanden et al., 2019).

As none of the earlier studies encompass ongoing circulations changes (Hanna et al., 2018) that also lead to the observed extreme melt events, and projections of weather and climate extremes are generally highly uncertain (Otto, 2016, 2019), our idealized experiments give a first estimate of the impact of future extreme events on the Greenland Ice Sheet. This initial estimate alone shows a major effect on ice retreat and sea-level rise and demonstrates the importance of including extremes in future sea-level rise projections.

https://doi.org/10.5194/tc-2022-145
Preprint. Discussion started: 11 August 2022

The Cryosphere
Discussions
Open Access
EGU

Figures

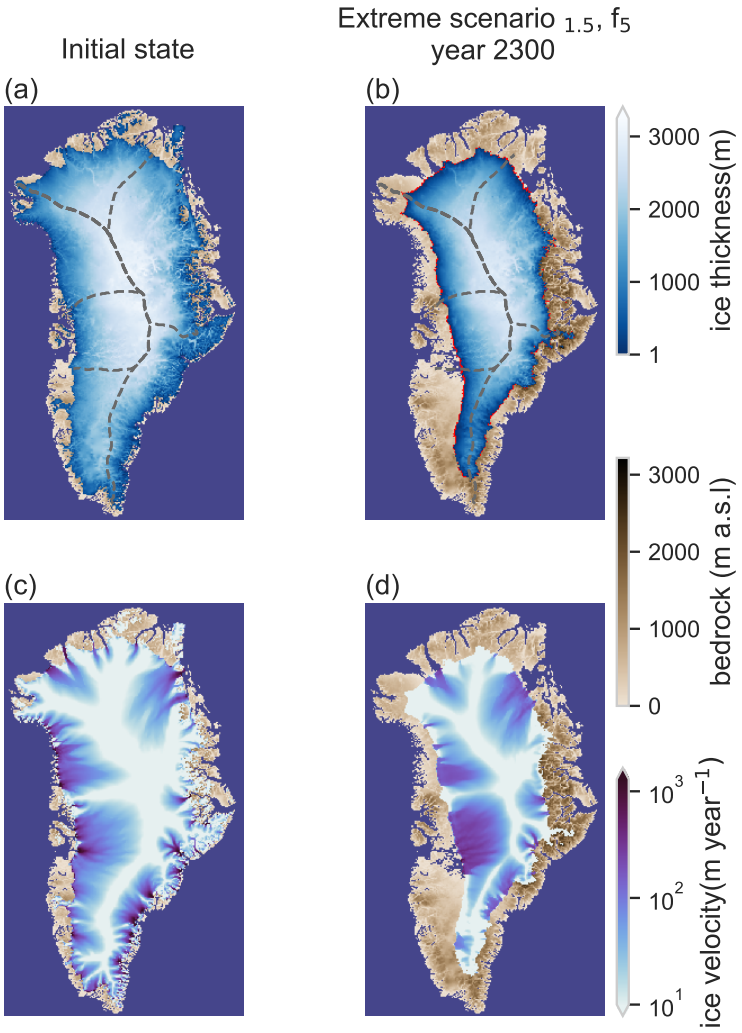

Figure 1. Additional ice loss caused by extreme events. (a) Ice thickness (in meters) of initial state with present-day boundary conditions and (c) the corresponding velocity field (in metres per year), as simulated with PISM. Basins are adjusted after (Rignot and Mouginot, 2012) by the IMBIE-2016 team (IMBIE2016, 2019). (b) Projected ice thickness distribution in the year 2300 under MIROC5 RCP8.5 temperature changes, including extreme events ($I_{1.5}, f_5$). Extremes are here applied by increasing the average temperature during the month of July by a factor of 1.5 every 5 years. Red margin indicates the additional area becoming ice-free due to extreme events compared to the MIROC5 RCP8.5 scenario without extremes. Brown shading illustrates the bedrock elevation (in metres above sea-level). (d) Corresponding velocity field in the year 2300 based on the scenario $I_{1.5}, f_5$.

https://doi.org/10.5194/tc-2022-145
Preprint. Discussion started: 11 August 2022

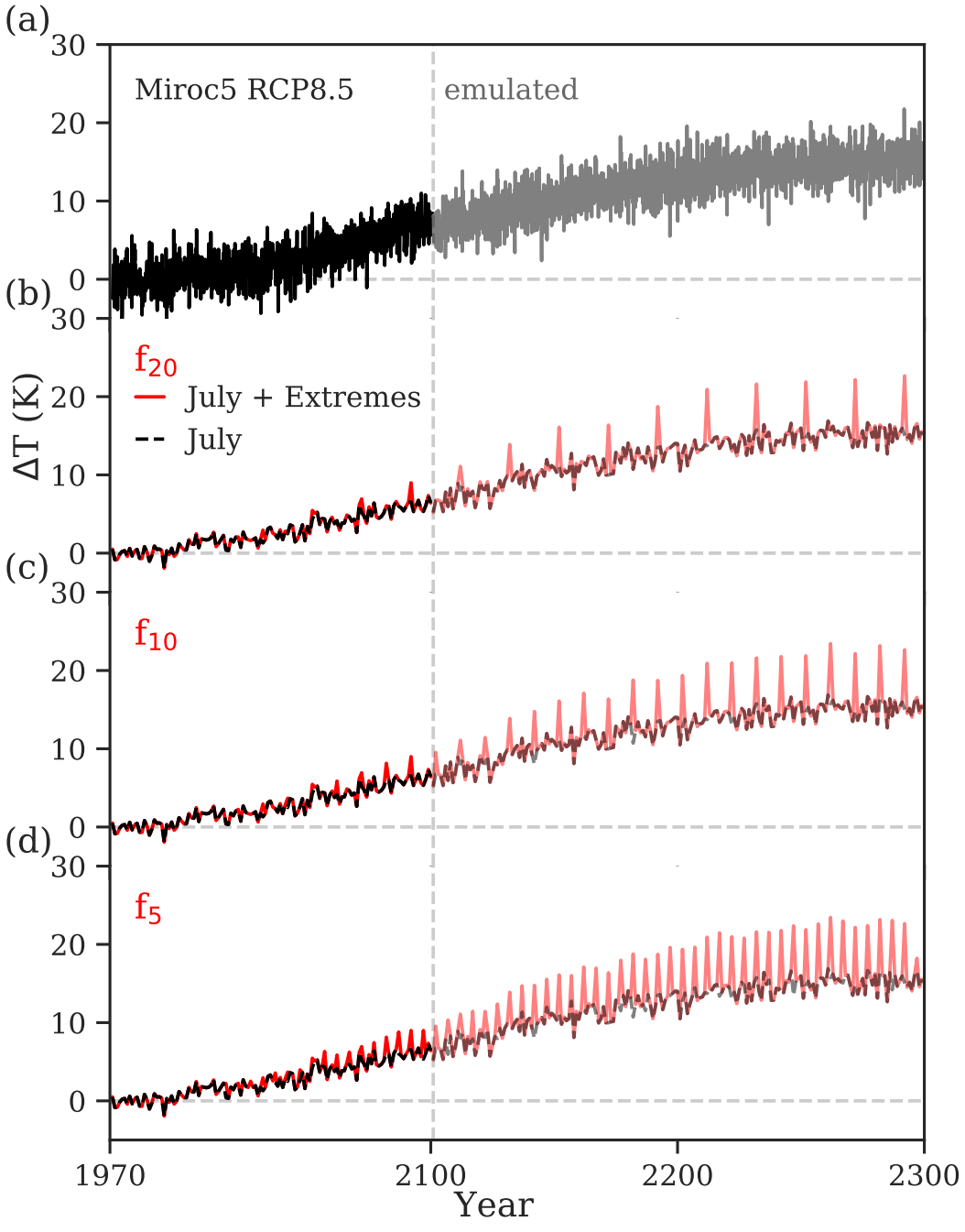

Figure 2. Temperature scenarios for the Greenland Ice Sheet. Given is the temperature anomaly over Greenland, based on the MIROC5 RCP8.5 projections, which is applied uniformly at the ice-sheet surface. (a) The forcing scenario without extremes on a monthly timescale (black, solid) from MIROC 5 projection until year 2100, and emulated (grey) thereafter (see Methods). (b)-(d) July temperature projection (black, dashed) including extremes (red) occurring every 20 (f_{20}), 10 (f_{10}) and 5 (f_5) years with an intensity of 1.5 times the 10-year running mean ($I_{1.5}$).

https://doi.org/10.5194/tc-2022-145
Preprint. Discussion started: 11 August 2022

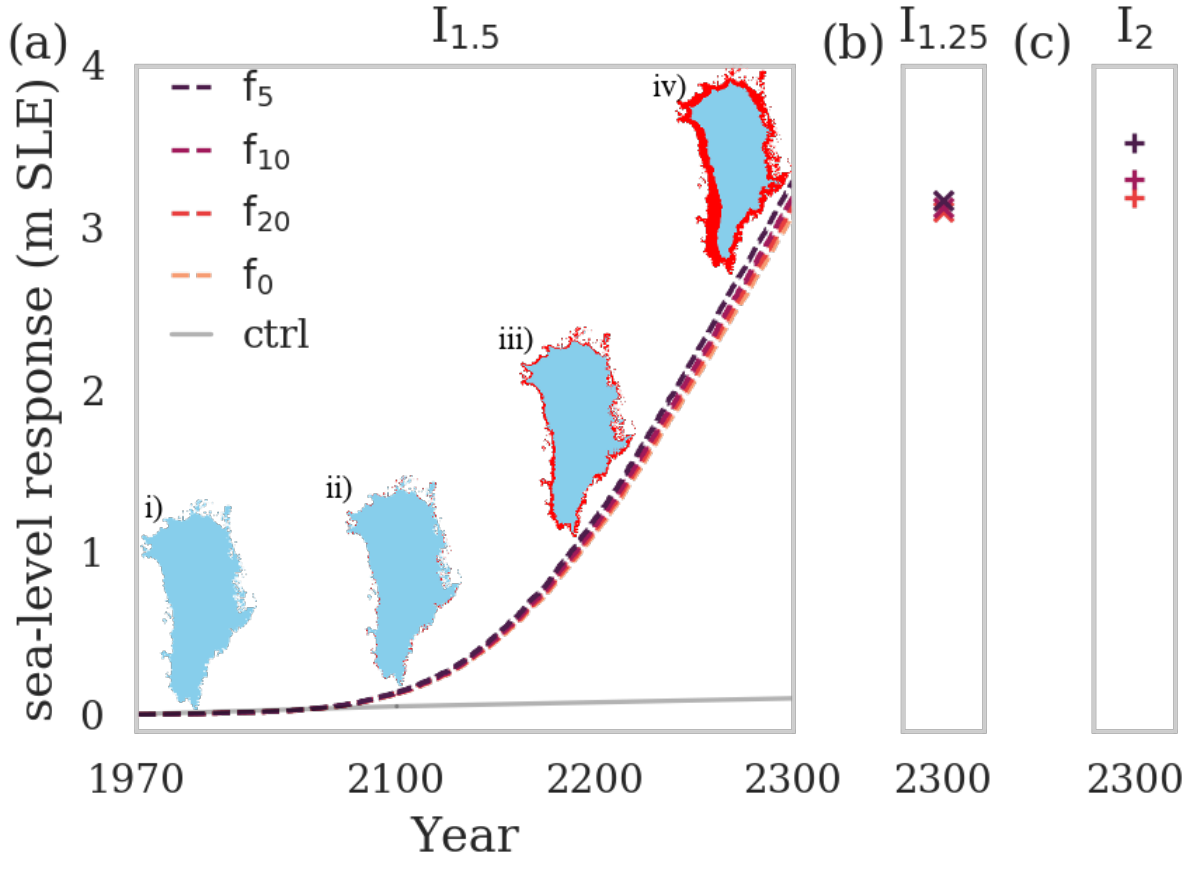

Figure 3. Sea-level rise contribution of the Greenland Ice Sheet until 2300. (a) Fully dynamic sea-level rise contribution until 2300 for the forcing scenario without (orange) and with extremes occurring every 20 (red), 10 (pink) and 5 (blue) years, with intensity $I_{1.5}$. Control run (light gray) is subtracted from all simulations. The corresponding ice sheet extent in 1971 (i) and the emerging ice retreat in years 2100 (ii), 2200 (iii) and 2300 (iv) are given in light blue and red shading, respectively. (b),(c) Sea level rise contribution by 2300 for the same experiments but less and more intense extremes of $I_{1.25}$ and I_5, respectively.

https://doi.org/10.5194/tc-2022-145
Preprint. Discussion started: 11 August 2022

The Cryosphere Discussions
Open Access
EGU

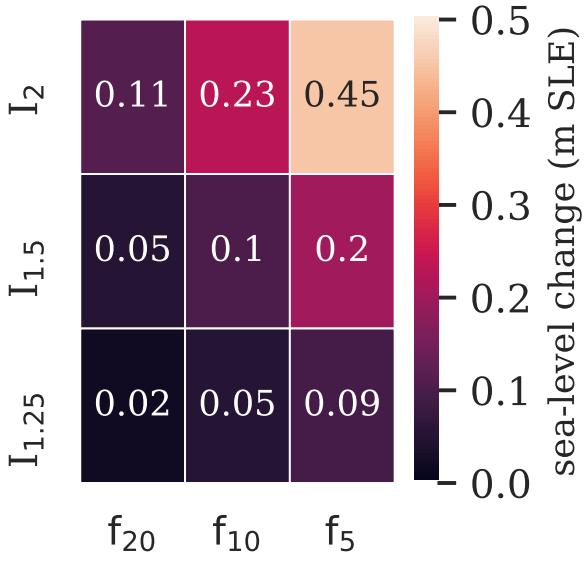

Figure 4. Importance of intensity and frequency of extremes. Given is the projected sea-level rise contribution in year 2300, including full ice dynamics, for each extreme scenario, subtracted by the sea-level rise scenario without extremes (MIROC5) in 2300 (see also SI, Table 2).

Tables

		f_0	f_{20}	f_{10}	f_5
$I_{1.25}$	SMB only	0.08m	0.08m	0.08m	0.09m
	dynamics, no s-e-f	0.11m	0.11m	0.11m	0.11m
	full dynamics	0.13m	0.13m	0.13m	0.13m
$I_{1.5}$	SMB only	0.08m	0.08m	0.09m	0.09m
	dynamics, no s-e-f	0.11m	0.11m	0.11m	0.12m
	full dynamics	0.13m	0.13m	0.13m	0.13m
I_2	SMB only	0.08m	0.09m	0.09m	0.10m
	dynamics, no s-e-f	0.11m	0.11m	0.12m	0.13m
	full dynamics	0.13m	0.13m	0.14m	0.15m

Table 1. Projected SLR in the year 2100 for experiments with different extreme event intensities ($I_{1.25}, I_{1.5}, I_2$) and frequencies every 20, 10 or 5 years (f_{20}, f_{10}, f_5). Projections without extremes are noted with f_0. For each combination of I and f, experiments were run allowing changes in SMB only, dynamics without the surface-elevation-feedback (s-e-f) and the full dynamics of the Greenland Ice Sheet.

https://doi.org/10.5194/tc-2022-145
Preprint. Discussion started: 11 August 2022

		f_0	f_{20}	f_{10}	f_5
$I_{1.25}$	SMB only	2.27m	2.29m	2.31m	2.34m
	dynamics, no s-e-f	2.31m	2.33m	2.35m	2.38m
	full dynamics	3.08m	3.10m	3.12m	3.17m
$I_{1.5}$	SMB only	2.27m	2.31m	2.35m	2.43m
	dynamics, no s-e-f	2.31m	2.35m	2.39m	2.47m
	full dynamics	3.08m	3.13m	3.18m	3.28m
I_2	SMB only	2.27m	2.36m	2.45m	2.62m
	dynamics, no s-e-f	2.31m	2.40m	2.48m	2.66m
	full dynamics	3.08m	3.19m	3.30m	3.52m

Table 2. Projected SLR in the year 2300 for experiments with different extreme event intensities ($I_{1.25}, I_{1.5}, I_2$) and frequencies every 20,10 or 5 years (f_{20}, f_{10}, f_5). Projections without extremes are noted with f_0. For each combination of I and f, experiments were run allowing changes in SMB only, dynamics without the surface-elevation-feedback (s-e-f) and the full dynamics of the Greenland Ice Sheet.

Code and data availability. This pism code used for this study is freely available at https://github.com/pism/pism/releases/tag/v1.1.3 The data from the MAR output is freely available at ftp://ftp.climato.be/fettweis/MARv3.9/ISMIP6/GrIS/ERA_1958-2017 and ftp://ftp.climato.be/fettweis/MARv3.9/ISMIP6/GrIS/ERA_1958-2017. The derived forcing data, spin-up state and scripts for the spin-up, control run, projection runs, and sea level rise calculation for the SMB only case are provided at https://doi.org/10.5281/zenodo.5162937.

Author contributions. R.W. conceived the study. J.B. and R.W. designed the study and conducted the analysis. J.B. performed the experiments, data processing, analysis and visualization. J.B. prepared the manuscript with contribution of R.W.

Competing interests. The authors declare no competing interests.

Acknowledgements. We thank Matthew Palmer for providing his emulated global mean temperature data set, Alison Delhasse and Xavier Fettweis for providing the monthly and daily MAR output fields of the CMIP5 MIROC5 RCP8.5 simulations. This work is supported by the Deutsche Forschungsgemeinschaft project 422877703. R.W. further acknowledges support by the European Union's Horizon 2020 research and innovation programme under grant agreements no. 820575 (TiPACCs) and 869304 (PROTECT). The authors gratefully acknowledge the European Regional Development Fund (ERDF), the German Federal Ministry of Education and Research and the Land Brandenburg

https://doi.org/10.5194/tc-2022-145
Preprint. Discussion started: 11 August 2022

for supporting this project by providing resources on the high performance computer system at the Potsdam Institute for Climate Impact Research.

https://doi.org/10.5194/tc-2022-145
Preprint. Discussion started: 11 August 2022

References

AMAP: Arctic Climate Change Update 2021: Key Trends and Impacts. Summary for Policy-makers., 2021.

Aschwanden, A., Bueler, E., Khroulev, C., and Blatter, H.: An enthalpy formulation for glaciers and ice sheets, Journal of Glaciology, 58, 441–457, https://doi.org/10.3189/2012JoG11J088, 2012.

Aschwanden, A., Fahnestock, M. A., and Truffer, M.: Complex Greenland outlet glacier flow captured, Nature Communications, 7, 10 524, 2016.

Aschwanden, A., Fahnestock, M. A., Truffer, M., Brinkerhoff, D. J., Hock, R., Khroulev, C., Mottram, R., and Khan, S. A.: Contribution of the Greenland Ice Sheet to sea level over the next millennium, Science Advances, 5, eaav9396, https://doi.org/10.1126/sciadv.aav9396, 2019.

Beckmann, J., Perrette, M., Beyer, S., Calov, R., Willeit, M., and Ganopolski, A.: Modeling the response of Greenland outlet glaciers to global warming using a coupled flow line–plume model, The Cryosphere, 13, 2281–2301, https://doi.org/10.5194/tc-13-2281-2019, 2019.

Bevis, M., Harig, C., Khan, S. A., Brown, A., Simons, F. J., Willis, M., Fettweis, X., van den Broeke, M. R., Madsen, F. B., Kendrick, E., Caccamise, D. J., van Dam, T., Knudsen, P., and Nylen, T.: Accelerating changes in ice mass within Greenland, and the ice sheet's sensitivity to atmospheric forcing, Proceedings of the National Academy of Sciences, 116, 1934–1939, https://doi.org/10.1073/pnas.1806562116, 2019.

Bueler, E. and Brown, J.: Shallow shelf approximation as a "sliding law" in a thermomechanically coupled ice sheet model, Journal of Geophysical Research: Solid Earth, 114, 1–21, https://doi.org/10.1029/2008JF001179, 2009.

Calov, R. and Greve, R.: A semi-analytical solution for the positive degree-day model with stochastic temperature variations, Journal of Glaciology, 51, 173–175, https://doi.org/10.3189/172756505781829601, 2005.

Calov, R., Beyer, S., Greve, R., Beckmann, J., Willeit, M., Kleiner, T., Rückamp, M., Humbert, A., and Ganopolski, A.: Simulation of the future sea level contribution of Greenland with a new glacial system model, Cryosphere, 12, 3097–3121, https://doi.org/10.5194/tc-12-3097-2018, 2018.

Church, J. A., Clark, P. U., Cazenave, A., Gregory, J. M., Jevrejeva, S., Levermann, A., Merrifield, M. A., Milne, G. A., Nerem, R. S., Nunn, P. D., Payne, A. J., Pfeffer, W. T., Unnikrishnan, D. S., and A.S.: Sea level change, Climate Change 2013: The Physical Science Basis. Contribution of Working Group I to the Fifth Assessment Report of the Intergovernmental Panel on Climate Change, pp. 1137–1216, https://doi.org/10.1017/CB09781107415315.026, 2013.

Cullather, R. I., Andrews, L. C., and Croteau, M. J.: Anomalous Circulation in July 2019 Resulting in Mass Loss on the Greenland Ice Sheet Geophysical Research Letters, pp. 1–10, https://doi.org/10.1029/2020GL087263, 2020.

Dee, D. P., Uppala, S. M., Simmons, A. J., Berrisford, P., Poli, P., Kobayashi, S., Andrae, U., Balmaseda, M. A., Balsamo, G., Bauer, P., Bechtold, P., Beljaars, A. C., van de Berg, L., Bidlot, J., Bormann, N., Delsol, C., Dragani, R., Fuentes, M., Geer, A. J., Haimberger, L., Healy, S. B., Hersbach, H., Hólm, E. V., Isaksen, L., Kållberg, P., Köhler, M., Matricardi, M., Mcnally, A. P., Monge-Sanz, B. M., Morcrette, J. J., Park, B. K., Peubey, C., de Rosnay, P., Tavolato, C., Thépaut, J. N., and Vitart, F.: The ERA-Interim reanalysis: Configuration and performance of the data assimilation system, Quarterly Journal of the Royal Meteorological Society, 137, 553–597, https://doi.org/10.1002/qj.828, 2011.

Delhasse, A., Fettweis, X., Kittel, C., Amory, C., and Agosta, C.: Brief communication: Impact of the recent atmospheric circulation change in summer on the future surface mass balance of the Greenland Ice Sheet, Cryosphere, 12, 3409–3418, https://doi.org/10.5194/tc-12-3409-2018, 2018.

https://doi.org/10.5194/tc-2022-145
Preprint. Discussion started: 11 August 2022

Dobricic, S., Russo, S., Pozzoli, L., Wilson, J., and Vignati, E.: Increasing occurrence of heat waves in the terrestrial Arctic, Environmental Research Letters, 15, https://doi.org/10.1088/1748-9326/ab6398, 2020.

Edwards, T. L., Fettweis, X., Gagliardini, O., Gillet-Chaulet, F., Goelzer, H., Gregory, J. M., Hoffman, M., Huybrechts, P., Payne, A. J., Perego, M., Price, S., A., Q., and Ritz, C.: Effect of uncertainty in surface mass balance–elevation feedback on projections of the future sea level contribution of the {Greenland} ice sheet, The Cryosphere, 8, 10.5194/tc–8–195–2014, https://doi.org/195-208, 2014.

Fettweis, X.: Monthly MARv3.9 outputs for ISMIP6 using EAR and ERA-Intermim, ftp://ftp.climato.be/fettweis/MARv3.9/ISMIP6/GrIS/ERA_1958-2017(2019), 2019a.

Fettweis, X.: Monthly MARv3.9 outputs for ISMIP6 using MIROC5-rcp85, ftp://ftp.climato.be/fettweis/MARv3.9/ISMIP6/GrIS/ERA_1958-2017 (2019), 2019b.

Fettweis, X., Franco, B., Tedesco, M., Van Angelen, J. H., Lenaerts, J. T., Van Den Broeke, M. R., and Gallée, H.: Estimating the Greenland ice sheet surface mass balance contribution to future sea level rise using the regional atmospheric climate model MAR, Cryosphere, 7, 469–489, https://doi.org/10.5194/tc-7-469-2013, 2013.

Fettweis, X., Box, J. E., Agosta, C., Amory, C., Kittel, C., Lang, C., Van As, D., Machguth, H., and Gallée, H.: Reconstructions of the 1900-2015 Greenland ice sheet surface mass balance using the regional climate MAR model, Cryosphere, 11, 1015–1033, https://doi.org/10.5194/tc-11-1015-2017, 2017.

Fox-Kemper, B., H. H. C. X. S. D. T. E. N. G. M. H. R. K. G. K. A. M. D. N. S. N. I. N. L. R. J.-B. S. A. S. and Yu, Y.: Ocean, Cryosphere and Sea Level Change, Climate Change 2013: The Physical Science Basis. Contribution of Working Group I to the Sixth Assessment Report of the Intergovernmental Panel on Climate Change [MassonDelmotte, V., P. Zhai, A. Pirani, S.L. Connors, C. Péan, S. Berger, N. Caud, Y. Chen, L. Goldfarb, M.I. Gomis, M. Huang, K. Leitzell, E. Lonnoy, J.B.R. Matthews, T.K. Maycock, T. Waterfield, O. Yelekçi, R. Yu, and B. Zhou (eds.)].Cambridge University Press. In Press, https://doi.org/10.1017/CB09781107415315.026, 2021.

Frederikse, T., Landerer, F., Caron, L., Adhikari, S., Parkes, D., Humphrey, V. W., Dangendorf, S., Hogarth, P., Zanna, L., Cheng, L., and Wu, Y. H.: The causes of sea-level rise since 1900, Nature, 584, 393–397, https://doi.org/10.1038/s41586-020-2591-3, 2020.

Fürst, J. J., Goelzer, H., and Huybrechts, P.: Ice-dynamic projections of the Greenland ice sheet in response to atmospheric and oceanic warming, The Cryosphere, 9, 1039–1062, https://doi.org/10.5194/tc-9-1039-2015, 2015.

Goelzer, H., Nowicki, S., Payne, A., Larour, E., Seroussi, H., Lipscomb, W. H., Gregory, J., Abe-Ouchi, A., Shepherd, A., Simon, E., Agosta, C., Alexander, P., Aschwanden, A., Barthel, A., Calov, R., Chambers, C., Choi, Y., Cuzzone, J., Dumas, C., Edwards, T., Felikson, D., Fettweis, X., Golledge, N. R., Greve, R., Humbert, A., Huybrechts, P., Le Clec'H, S., Lee, V., Leguy, G., Little, C., Lowry, D., Morlighem, M., Nias, I., Quiquet, A., Rückamp, M., Schlegel, N. J., Slater, D. A., Smith, R., Straneo, F., Tarasov, L., Van De Wal, R., and Van Den Broeke, M.: The future sea-level contribution of the Greenland ice sheet: A multi-model ensemble study of ISMIP6, Cryosphere, 14, 3071–3096, https://doi.org/10.5194/tc-14-3071-2020, 2020.

Hanna, E., Huybrechts, P., Steffen, K., Cappelen, J., Huff, R., Shuman, C., Irvine-Fynn, T., Wise, S., and Griffiths, M.: Increased runoff from melt from the Greenland Ice Sheet: A response to global warming, Journal of Climate, 21, 331–341, https://doi.org/10.1175/2007JCLI1964.1, 2008.

Hanna, E., Fettweis, X., and Hall, R. J.: Brief communication: Recent changes in summer Greenland blocking captured by none of the CMIP5 models, Cryosphere, 12, 3287–3292, https://doi.org/10.5194/tc-12-3287-2018, 2018.

Hofer, S., Tedstone, A. J., Fettweis, X., and Bamber, J. L.: Decreasing cloud cover drives the recent mass loss on the Greenland Ice Sheet, Science Advances, 3, https://doi.org/10.1126/sciadv.1700584, 2017.

Hutter, K.: Theoretical Glaciology; Material Science of Ice and the Mechanics of Glaciers and Ice Sheets, d. Reidel Publishing Company, Dordrecht, The Netherlands.(1983).

Huybrechts, P.: Sea-level changes at the LGM from ice-dynamic reconstructions of the Greenland and Antarctic ice sheets during the glacial cycles, Quaternary Science Reviews, 21, 203–231, https://doi.org/10.1016/S0277-3791(01)00082-8, 2002.

IMBIE2016: Rignot Drainage Basins, http://imbie.org/imbie-2016/drainage-basins/GRE_Basins_IMBIE2_v1.3 (2019), 2019.

Johnson, J., Hand, B., and Bocek, T.: Greenland Standard Data Set, http://websrv.cs.umt.edu/isis/index.php/Present_Day_Greenland/Greenland_5km_v1.1.nc (2019).

Joughin, I., Smith, B. E., and Howat, I. M.: A complete map of Greenland ice velocity derived from satellite data collected over 20 years, Journal of Glaciology, 64, 1–11, https://doi.org/10.1017/jog.2017.73, 2018.

King, M. D., Howat, I. M., Candela, S. G., Noh, M. J., Jeong, S., Noël, B. P. Y., Broeke, M. R. V. D., Wouters, B., and Negrete, A.: Dynamic ice loss from the Greenland Ice Sheet driven by sustained glacier retreat, Communications Earth & Environment, pp. 1–7, https://doi.org/10.1038/s43247-020-0001-2, 2020.

Krebs-Kanzow, U., Gierz, P., and Lohmann, G.: Brief communication: An ice surface melt scheme including the diurnal cycle of solar radiation, Cryosphere, 12, 3923–3930, https://doi.org/10.5194/tc-12-3923-2018, 2018.

Le Clec'h, S., Charbit, S., Quiquet, A., Fettweis, X., Dumas, C., Kageyama, M., Wyard, C., and Ritz, C.: Assessment of the Greenland ice sheet-atmosphere feedbacks for the next century with a regional atmospheric model coupled to an ice sheet model, Cryosphere, 13, 373–395, https://doi.org/10.5194/tc-13-373-2019, 2019.

Mikkelsen, T. B., Grinsted, A., and Ditlevsen, P.: Influence of temperature fluctuations on equilibrium ice sheet volume, The Cryosphere, 12, 39–47, https://doi.org/10.5194/tc-12-39-2018, 2018.

Morland, L. W.: Unconfined ice-shelf flow, in: C. J. van der Veen and J. Oerlemans (Eds.), Dynamics of the West Antarctic Ice Sheet, pp. 99–116. D. Reidel Publishing Company, Dordrecht, The Netherlands.(1987).

Morlighem, M., Williams, C. N., Rignot, E., An, L., Arndt, J. E., Bamber, J. L., Catania, G., Chauché, N., Dowdeswell, J. A., Dorschel, B., Fenty, I., Hogan, K., Howat, I., Hubbard, A., Jakobsson, M., Jordan, T. M., Kjeldsen, K. K., Millan, R., Mayer, L., Mouginot, J., Noël, B. P., O'Cofaigh, C., Palmer, S., Rysgaard, S., Seroussi, H., Siegert, M. J., Slabon, P., Straneo, F., van den Broeke, M. R., Weinrebe, W., Wood, M., and Zinglersen, K. B.: BedMachine v3: Complete Bed Topography and Ocean Bathymetry Mapping of Greenland From Multibeam Echo Sounding Combined With Mass Conservation, https://doi.org/10.1002/2017GL074954, 2017.

Mouginot, J., Rignot, E., Bjørk, A. A., van den Broeke, M., Millan, R., Morlighem, M., Noël, B., Scheuchl, B., and Wood, M.: Forty-six years of Greenland Ice Sheet mass balance from 1972 to 2018, Proceedings of the National Academy of Sciences of the United States of America, 116, 9239–9244, https://doi.org/10.1073/pnas.1904242116, 2019.

Nghiem, S. V., Hall, D. K., Mote, T. L., Tedesco, M., Albert, M. R., Keegan, K., Shuman, C. A., DiGirolamo, N. E., and Neumann, G.: The extreme melt across the Greenland ice sheet in 2012, Geophysical Research Letters, 39, 6–11, https://doi.org/10.1029/2012GL053611, 2012.

Noël, B., Van De Berg, W. J., Van Wessem, J. M., Van Meijgaard, E., Van As, D., Lenaerts, J. T., Lhermitte, S., Munneke, P. K., Smeets, C. J., Van Ulft, L. H., Van De Wal, R. S., and Van Den Broeke, M. R.: Modelling the climate and surface mass balance of polar ice sheets using RACMO2 - Part 1: Greenland (1958-2016), Cryosphere, 12, 811–831, https://doi.org/10.5194/tc-12-811-2018, 2018.

Otto, F.: Attribution of extreme weather events: how does climate change affect weather?, Weather, 74, 325–326, https://doi.org/10.1002/wea.3610, 2019.

Otto, F. E.: Extreme events: The art of attribution, Nature Climate Change, 6, 342–343, https://doi.org/10.1038/nclimate2971, 2016.

Overland, J. E. and Wang, M.: The 2020 Siberian heat wave, International Journal of Climatology, 41, E2341–E2346, https://doi.org/10.1002/joc.6850, 2021.

Palmer, M. D., Harris, G. R., and Gregory, J. M.: Extending CMIP5 projections of global mean temperature change and sea level rise due to thermal expansion using a physically-based emulator, Environmental Research Letters, 13, https://doi.org/10.1088/1748-9326/aad2e4, 2018.

Rahmstorf, S. and Coumou, D.: Increase of extreme events in a warming world, Proceedings of the National Academy of Sciences, 108, 17 905–17 909, https://doi.org/10.1073/pnas.1101766108, 2011.

Rignot, E. and Mouginot, J.: Ice flow in Greenland for the International Polar Year 2008-2009, Geophysical Research Letters, 39, 1–7, https://doi.org/10.1029/2012GL051634, 2012.

Shannon, S. R., Payne, A. J., Bartholomew, I. D., Van Den Broeke, M. R., Edwards, T. L., Fettweis, X., Gagliardini, O., Gillet-Chaulet, F., Goelzer, H., Hoffman, M. J., Huybrechts, P., Mair, D. W., Nienow, P. W., Perego, M., Price, S. F., Paul Smeets, C. J., Sole, A. J., Van De Wal, R. S., and Zwinger, T.: Enhanced basal lubrication and the contribution of the Greenland ice sheet to future sea-level rise, Proceedings of the National Academy of Sciences of the United States of America, 110, 14 156–14 161, https://doi.org/10.1073/pnas.1212647110, 2013.

Shepherd, A., Ivins, E., Rignot, E., Smith, B., van den Broeke, M., Velicogna, I., Whitehouse, P., Briggs, K., Joughin, I., Krinner, G., Nowicki, S., Payne, T., Scambos, T., Schlegel, N., A, G., Agosta, C., Ahlstrøm, A., Babonis, G., Barletta, V. R., Bjørk, A. A., Blazquez, A., Bonin, J., Colgan, W., Csatho, B., Cullather, R., Engdahl, M. E., Felikson, D., Fettweis, X., Forsberg, R., Hogg, A. E., Gallee, H., Gardner, A., Gilbert, L., Gourmelen, N., Groh, A., Gunter, B., Hanna, E., Harig, C., Helm, V., Horvath, A., Horwath, M., Khan, S., Kjeldsen, K. K., Konrad, H., Langen, P. L., Lecavalier, B., Loomis, B., Luthcke, S., McMillan, M., Melini, D., Mernild, S., Mohajerani, Y., Moore, P., Mottram, R., Mouginot, J., Moyano, G., Muir, A., Nagler, T., Nield, G., Nilsson, J., Noël, B., Otosaka, I., Pattle, M. E., Peltier, W. R., Pie, N., Rietbroek, R., Rott, H., Sandberg Sørensen, L., Sasgen, I., Save, H., Scheuchl, B., Schrama, E., Schröder, L., Seo, K. W., Simonsen, S. B., Slater, T., Spada, G., Sutterley, T., Talpe, M., Tarasov, L., van de Berg, W. J., van der Wal, W., van Wessem, M., Vishwakarma, B. D., Wiese, D., Wilton, D., Wagner, T., Wouters, B., and Wuite, J.: Mass balance of the Greenland Ice Sheet from 1992 to 2018, Nature, 579, 233–239, https://doi.org/10.1038/s41586-019-1855-2, 2020.

Slater, T., Hogg, A. E., and Mottram, R.: Ice-sheet losses track high-end sea-level rise projections, Nature Climate Change, https://doi.org/10.1038/s41558-020-0893-y, 2020.

Sullivan, R.: 'Mindboggling' Arctic heatwave breaks records. https://www.independent.co.uk/climate-change/news/arctic-temperature-map-iceland-heatwave-b1852984.html, TheGuardian, https://www.independent.co.uk/climate-change/news/arctic-temperature-map-iceland-heatwave-b1852984.html, 2021-11-10.

Taylor, K. E., Stouffer, R. J., and Meehl, G. A.: An overview of CMIP5 and the experiment design, Bulletin of the American Meteorological Society, 93, 485–498, https://doi.org/10.1175/BAMS-D-11-00094.1, 2012.

Tedesco, M. and Fettweis, X.: Unprecedented atmospheric conditions (1948-2019) drive the 2019 exceptional melting season over the Greenland ice sheet, Cryosphere, 14, 1209–1223, https://doi.org/10.5194/tc-14-1209-2020, 2020.

Tedesco, M., Fettweis, X., Van Den Broeke, M. R., Van De Wal, R. S., Smeets, C. J., Van De Berg, W. J., Serreze, M. C., and Box, J. E.: The role of albedo and accumulation in the 2010 melting record in Greenland, Environmental Research Letters, 6, https://doi.org/10.1088/1748-9326/6/1/014005, 2011.

Tedesco, M., Mote, T., Fettweis, X., Hanna, E., Jeyaratnam, J., Booth, J. F., Datta, R., and Briggs, K.: Arctic cut-off high drives the poleward shift of a new Greenland melting record, Nature Communications, 7, 1–6, https://doi.org/10.1038/ncomms11723, 2016.

https://doi.org/10.5194/tc-2022-145
Preprint. Discussion started: 11 August 2022

Tedstone, A. J., Nienow, P. W., Gourmelen, N., Dehecq, A., Goldberg, D., and Hanna, E.: Decadal slowdown of a land-terminating sector of the Greenland Ice Sheet despite warming, Nature, 526, 692–695, https://doi.org/10.1038/nature15722, 2015.

University of Alaska Fairbanks: Parallel Ice Sheet Model, https://github.com/pism/pism/releases/tag/v1.1.3 (2019), 2019.

Van Den Broeke, M. R., Enderlin, E. M., Howat, I. M., Kuipers Munneke, P., Noël, B. P., Jan Van De Berg, W., Van Meijgaard, E., and Wouters, B.: On the recent contribution of the Greenland ice sheet to sea level change, Cryosphere, 10, 1933–1946, https://doi.org/10.5194/tc-10-1933-2016, 2016.

Van Tricht, K., Lhermitte, S., Lenaerts, J. T., Gorodetskaya, I. V., L'Ecuyer, T. S., Noël, B., Van Den Broeke, M. R., Turner, D. D., and Van Lipzig, N. P.: Clouds enhance Greenland ice sheet meltwater runoff, Nature Communications, 7, https://doi.org/10.1038/ncomms10266, 2016.

van Vuuren, D. P., Edmonds, J., Kainuma, M., Riahi, K., Thomson, A., Hibbard, K., Hurtt, G. C., Kram, T., Krey, V., Lamarque, J. F., Masui, T., Meinshausen, M., Nakicenovic, N., Smith, S. J., and Rose, S. K.: The representative concentration pathways: An overview, Climatic Change, 109, 5–31, https://doi.org/10.1007/s10584-011-0148-z, 2011.